ZINC-LOADED CELLULOSE ACETATE MEMBRANES WITH POTENTIAL BIOMEDICAL APPLICATIONS

Mădălina OPREA[1], Anton FICAI[2*], Cornelia ILIE[3], Roxana TRUȘCĂ[4], Ovidiu Cristian OPREA[5], Oana Steluța ȘERBĂNESCU[1], Ștefan Ioan VOICU[6]

This study presents the successful synthesis of zinc-loaded cellulose acetate membranes with antibacterial properties and potential biomedical applications. The main goal of this research was to obtain hybrid materials via in situ synthesis of zinc-based compounds on the polymeric membranes surface, using a facile method based on impregnation with zinc salts and alkaline precipitation. FT-IR and SEM analysis were used to reveal the morpho-structural features, and the thermal stability was investigated by TGA and DSC. The swelling degree and antibacterial properties were also studied to determinate if the obtained membranes are suitable for use in the wound healing area.

Keywords: cellulose acetate, zinc oxide, hybrid membranes, wound dressings.

1. Introduction

In the context of an increased frequency of infections caused by antibiotics-resistant microorganisms [1], antibacterial materials containing alternative therapeutic agents such as metal oxide nanoparticles [2, 3], essential oils [4] or bio-extracts [5-7], attracted a lot of interest, especially in the wound healing area [8]. Besides the antimicrobial properties, wound dressings should also meet basic requirements such as biocompatibility, high fluid retention ability, allowance of gaseous exchanges and non-adherence to prevent auxiliary injury upon removal [9, 10]. Both synthetic and natural polymers can be used as wound dressings, nonetheless, the biocompatibility and biodegradability along with the physico-chemical and biomimetic features of biopolymers make them an optimal choice for such applications [11].

Cellulose remarked itself amongst biopolymers due to its high availability and notable properties such as biocompatibility, biodegradability, renewability, environmental friendliness and non-toxicity [10, 12-17]**.** However, its limited solubility in common organic solvents is a major disadvantage because it implies poor processability. Processability is an important feature of the polymers used in biomedical applications because, if the material possesses the requirements for usage in this field (e.g. biocompatibility, low toxicity, bioactivity, etc.), but is not easily and economically processible, so that the end product is cost effective, stable and homogeneous, then, the material is often discarded or replaced with a more suitable option.

A viable alternative to pure cellulose is represented by cellulose derivatives which maintain the benefic properties of cellulose and also have a good dissolution ability [18, 19]. Cellulose acetate (CA) is a cellulose ester that was widely researched especially for the production of polymeric membranes for water purification [20] and biomedical applications [21]. In virtue of its good mechanical properties, hydrophilicity [22] and leukocytes chemotactic character [23], cellulose acetate was considered an appropriate polymer for the production of wound healing mats.

Zinc is a well-known antimicrobial agent [24], its antibacterial mechanisms involving reactive oxygen species formation, Zn^{2+} ions liberation and direct contact between particles and cell membranes [25]. Zinc oxide (ZnO) particularly, owning to its role in fibroblast proliferation and angiogenesis, was frequently used as an active ingredient in wound dressings [25, 26]. Recent studies showed that zinc salts were also effective against a variety of pathogens and presented low toxicity towards human cells. Moreover, textile treatments with zinc salts were longer-lasting than ZnO colloidal dispersions and alcohol-based formulations due to the stronger chemical bonds formed between the hydrolyzed salts and the polymer chain [27]. Therefore, loading polymeric materials with aqueous solutions of zinc salts could be a novel, effective technique to provide them an antibacterial character, without affecting their properties or structure.

The purpose of this study was to obtain antibacterial cellulose acetate/zinc membranes, using a facile one-pot synthesis method based on alkaline precipitation of zinc salts, in situ, on the membranes surface. Following this treatment, it is expected that the membranes will be loaded with a combination of zinc-based compounds with antibacterial action and low toxicity to human epidermal cells, these characteristics recommending them for biomedical applications such as wound healing mats.

2. Materials and methods

2.1 Preparation of the hybrid membranes

Three zinc salt solutions were prepared by dissolving different percentages (1, 2 and 5%) zinc acetate dihydrate (Lach Ner, Czech Republic) in distilled water, under magnetic stirring at room temperature. The commercial cellulose acetate membranes (Prat Dumas, France) were placed in Petri dishes containing 10 ml of the corresponding zinc acetate solution or distilled water in the case of the neat sample. Diluted ammonium hydroxide (28-30%, Sigma Aldrich) was uniformly pulverized over the membranes to initiate the precipitation of zinc compounds and to ensure the deacetylation of cellulose acetate, thus favoring the interactions between the cellulosic matrix and the zinc compounds formed by alkaline precipitation. After 24 hours of impregnation, the modified membranes were dried at 80°C in a vacuum laboratory oven to remove excess moisture and residual solvents.

2.2 Characterization of the hybrid membranes

FT-IR spectra were recorded using a Nicolet 6700 spectrometer (Thermo Nicolet, Wiscounsin, United States of America) using 32 sample scans at a resolution of 4 cm^{-1} in the 400 - 4000 cm^{-1} interval.

Thermogravimetric analysis (TGA) was realized using a Netzsch STA 449C Jupiter (Netzsch, Selb, Germany) thermal analyzer. The samples were placed in alumina crucibles and heated with 10 °C/min from room temperature to 900 °C, under an air flow of 50 ml/min.

Differential scanning calorimetry (DSC) analysis was carried out on a DSC Q2000 (TA Instruments, New Castle, United States of America) under a helium flow of 25 ml/min. The samples were packed in alumina crucibles and cooled to 5 °C, held at that temperature for 2 min to delete the thermal history, then heated at 300 °C with a constant rate of 10 °C/min.

Scanning electron microscopy was performed using an Inspect F Quanta analyzer with 1.2 nm resolution (FEI-Philips, Netherlands), equipped with an energy dispersive X-ray (EDX) spectrometer with a resolution of 133 eV at MnK. The images were obtained by recording the secondary electron beam resulted, with an energy of 30 keV.

The swelling degree and swelling kinetics were determined through a conventional gravimetric method. The dried materials were cut into small rectangles of 10×5 mm and weighed. Afterwards, they were completely immersed in vials filled with 1.5 ml of distilled water. At predetermined time points – 0.5, 1, 2, 4, 6, 24 and 48 hours – the samples were taken and gently wiped to remove excess water present on the surface. The swollen membranes were weighed until a

constant value was noticed, and the swelling degree at each time point was calculated using the following equation:

$$Swelling\ degree\ [\%] = \frac{mf\ [mg] - mi\ [mg]}{mi\ [mg]} \times 100$$

where *mf* is the weight of the swollen sample and *mi* is the weight of the dry sample.

The biological characterization consisted in three types of antimicrobial assessments, qualitative, quantitative and semi-quantitative, performed on two different bacterial strains *Gram-positive Staphylococcus aureus* and *Gram-negative Pseudomonas aeruginosa*. For the qualitative assessment, a standardized inoculum, represented by a suspension of microbial cells in physiological sterile water, was seeded on the surface of a 2% agarose gel medium (pH = 7.2-7.4). The samples were cut in approximately equal size disks (6 mm diameter) and placed in the Petri dishes containing the seeded microbial suspensions. To avoid the impact of external contaminants over the experiment, the samples were previously sterilized under UV radiations for 30 minutes. The plates were incubated for 16-18 h at 37 °C to allow the development of microorganisms and the diffusion of antibacterial compounds from the tested materials. The results were interpreted by evaluating the diameter of the growth inhibition areas. The semi-quantitative assessment of antimicrobial activity consisted in evaluating the samples' effect on microorganism's development in planktonic cultures. The UV sterilized samples were deposited in a well plate with 96 sterile wells; 150 µL of liquid Boulion medium and 15 µL of bacterial suspension were added over them. The well plates were incubated for 16-18 h at 37 °C. At the end of the incubation time the turbidity of the resulting microbial suspension was measured spectrophotometrically at 620 nm. The quantitative assessment of antimicrobial activity was performed using the previously tested well plates. 1 µL of microbial suspension was collected from each well and inoculated on the surface of a 2% agarose gel medium, using a calibrated loop, in order to quantitatively determinate the number of microbial cells expressed in colony forming units/ml (CFU/ml). The test was realized in triplicate and the number of viable cells was evaluated after 24 h of incubation at 37 °C.

3. Results and discussion

3.1 FT-IR

In the FT-IR spectrum of the neat CA membrane, the peaks characteristic to this polymer can be observed at 1740, 1372 and 1277 cm^{-1}, generated by the C=O stretching of the ester group, the C–H bond in −OCOCH3 group and the −CO− stretching band of acetyl group [28]. The peak corresponding to the ester group is not sharp and well defined, this indicating that the ammonia hydroxide

treatment initiated the deacetylation of the CA membrane [29]. The broad peak between 3600 – 3100 cm^{-1} and the two smaller peaks at 2975 cm^{-1} and 2916 cm^{-1} belong to the –OH and CH_2 stretching modes. The peak at 1643 cm^{-1} is generated by the bending mode of the physically adsorbed water and the ones observed at 1160 and 1061 cm^{-1} are characteristic to materials based on cellulose, being associated with the C–O antisymmetric bridge stretching and C–O–C pyranose ring skeletal vibration respectively [30].

After impregnation with the zinc salt /ammonia hydroxide solution, the ester group of CA (1740 cm^{-1}) has a decreased intensity, resembling more likely to a shoulder in the spectra of the zinc loaded membranes. This, paired with the intense additional peak at 1712 cm^{-1}, associated to free acetate groups, indicate on one hand the partial deacetylation of the CA membrane and on the other hand the hydrolysis of the zinc acetate, CH_3COO^- ions resulting from both processes [31]. In the FT-IR spectra of the zinc modified membranes, starting with a 2% zinc concentration, additional peaks are present at 1554 cm^{-1} and 1436 cm^{-1}. The peaks are characteristic to the symmetric and antisymmetric vibrations of the carboxyl groups in the structure of zinc acetate [32]. These peaks along with the narrowing and shifting of the hydroxyl peak towards lower values (3400 - 3000 cm^{-1}) confirm the interactions between zinc ions and the hydroxyl groups of the partially deacetylated CA membrane. The increased intensity of the –OH corresponding peak could also be generated by the formation of large quantities of $Zn(OH)_2$ due to an excess of ammonium hydroxide in the reaction solution [33].

According to the mechanism proposed by Thein et al. the main compounds that can be formed following the interaction between Zn^{2+} ions, dissociated from zinc acetate and OH^- and NH^{4+} ions, resulted from the hydrolysis of ammonia hydroxide, are zinc hydroxide $Zn(OH)_2$ and complex ions such as tetraaminezincate $[Zn(NH_3)_4]^{2+}$ and tetrahydroxozincate $[Zn(OH)_4]^{2-}$ that further contribute to the growth of zinc oxide nuclei [34]. At 5% zinc concentration, the sharp peak at 952 cm^{-1} and the increased intensity of the peaks at 724, 692 and 621 cm^{-1} suggest the formation of zinc hydroxide [35] and complex tetraaminezincate ions [36] in the CA membrane structure. Some additional peaks can also be observed at 509 and 423 cm^{-1}; according to previous literature studies these could be attributed to Zn-O bonds in zinc oxide structure [37].

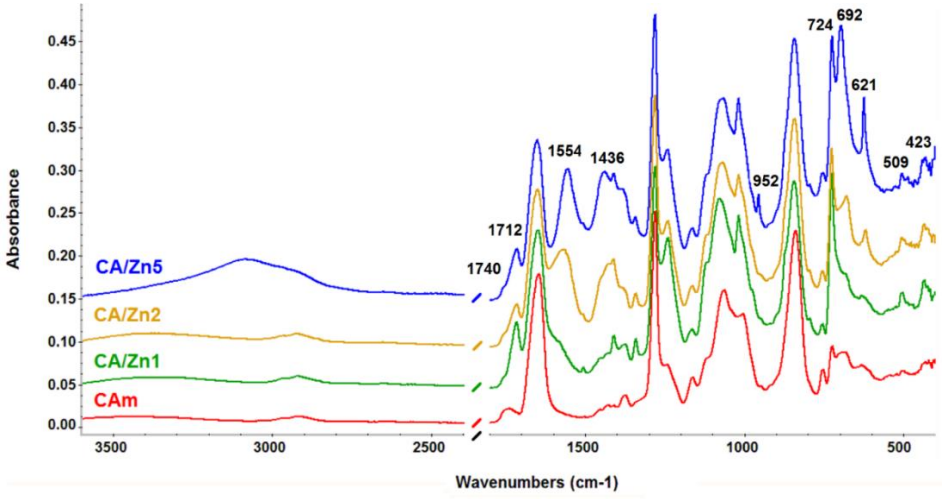

Fig. 1. FT-IR spectra of the CA membranes.

3.2 TGA, DTG

The TGA curve obtained for the neat CA membrane (Fig. 2a) reveals that the material degradation occurs in three steps, characteristic for cellulose-based materials [38]. The first weight loss takes place between 25 and 320 °C and is associated with dehydration and evaporation of volatile molecules, such as unreacted ammonia hydroxide, from the membrane structure. The main weight loss related to the degradation of the cellulose acetate chains is observed in the 320 – 460 °C interval [39]. The carbonization of the degradation products into ash takes place after 460 °C with a maximum at 502 °C, practically zero residual mass being recorded at the end of the process. The changes in the thermal degradation behavior of the CA/Zn5 membrane compared to the neat CA are best observed in the DTG curves (Fig. 2b). A small additional evaporation peak is present in the 45 – 75 °C interval, associated to the dehydration of unreacted zinc acetate dihydrate, the resulting product being anhydrous zinc acetate [40]. The evaporation peak is slightly shifted towards lower values, this indicating a higher volatility of the eliminated compounds. The degradation of the polymeric structure takes place in the same temperature interval (320 – 460 °C), however the maximum degradation rate is recorded at lower temperatures (419 °C) compared to the neat sample (436 °C). The carbonization process is strongly exothermic with a maximum at 572 °C and it is divided in two steps represented by a sharp peak followed by a narrow shoulder. The increase of the temperature corresponding to the maximum carbonization rate correlated to the dual-step thermal transformation could indicate that the resulted degradation product contains a large fraction of cellulose acetate – zinc compounds organic complexes that carbonize prior to the pure CA

chains. The residual mass of 2.8% indicates the content of inorganic zinc oxide in the membrane structure.

Table 1

The thermal degradation behavior of the CA membranes.

	Dehydration and evaporation			Degradation			Carbonization			
Sample	Temperature interval [°C]	Peak max [°C]	Weight loss [%]	Temperature interval [°C]	Peak max [°C]	Weight loss [%]	Temperature interval [°C]	Peak max [°C]	Weight loss [%]	Residue [%]
CAm	25 - 320	208	15.08	320 - 460	436	74.88	460 - 600	502	9.69	0.18
CA/Zn 5	25 – 320	200	16.14	320 - 460	419	66.58	460 - 600	572	14.20	2.80

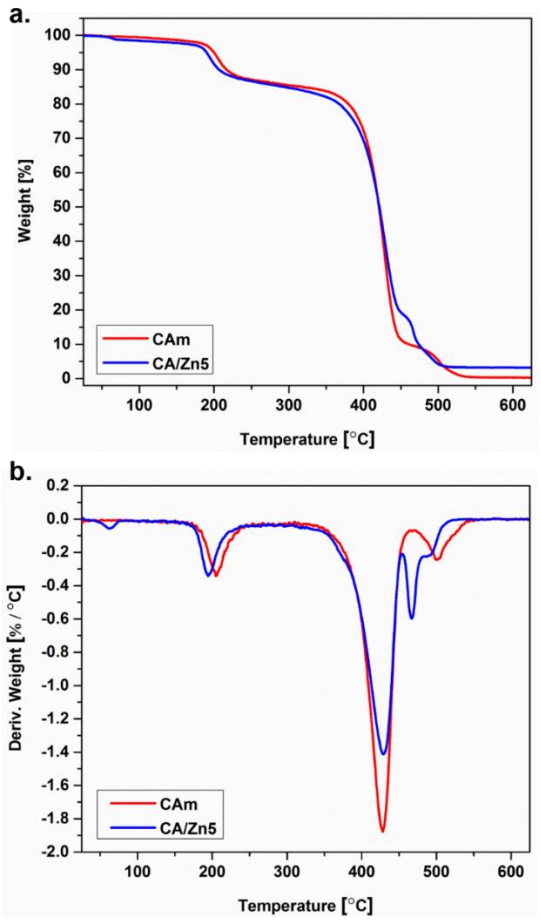

Fig. 2. Thermogravimetric analysis - TGA (a) and derivative thermogravimetric – DTG (b) curves of the CA membranes.

3.3 DSC

In the DSC curve obtained for the neat cellulose acetate membrane, three major events can be noticed. Upon heating, the polymer turns from a hard, glassy

material to a soft, rubbery one and the glass transition temperature appears at 81 °C. The broad exothermic peak at 206 °C represents the crystallization that occurs because the polymeric chains are more flexible due to the increased temperature and are able to organize in ordered structures called crystals. Fusion begins at 244 °C and reaches maximum intensity at 251 °C. This phenomenon is visible in the DSC curve as a narrow endothermic peak. The presence of both glass transition and fusion in the DSC curve indicates the fact that the polymer is comprised of amorphous and crystalline phases. For the membrane modified with the 5% zinc salt solution, an additional endothermic peak appears between 49 and 75 °C, this was attributed to the evaporation of excess water and volatile ammonia hydroxide residues from the membrane structure combined with the dehydration of unreacted zinc acetate dihyrate. The membrane modification did not influence the glass transition temperature which remains unchanged. However, the crystallization enthalpy has a lower value and the peaks corresponding to crystallization and fusion become broader compared to the neat CA membrane; this could be related to a wider crystal size distribution and a lower degree of organization, aspect also observed in the SEM images.

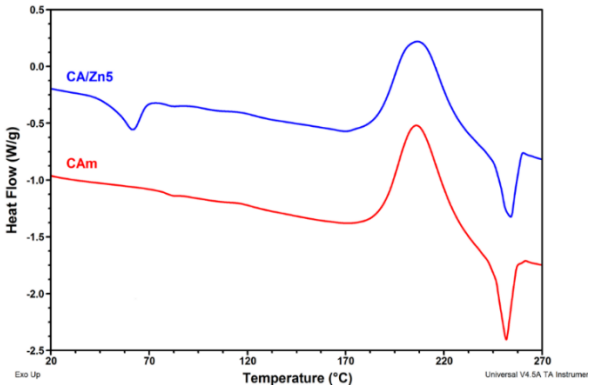

Fig. 3. DSC curves of the CA membranes – neat (CAm) and 5% zinc (CA/Zn5).

Table 2

Thermal characteristics of the analyzed membranes.

Sample	**Glass transition temperature - Tg [°C]**	**Crystallization temperature - Tc [°C]**	**Enthalpy of crystallization - ΔHc [J/g]**	**Fusion Temperature - Tf [°C]**
CAm	81	206	169	251
CA/Zn5	81	207	157	253

The crystallinity percentage of the membranes can be calculated using the ratio between the enthalpy of fusion of the analyzed sample (ΔHf) and the enthalpy of fusion of a perfect crystal of that material (ΔHf_o). Considering the fact

that ΔHf_o of cellulose acetate has the value of 58.8 J/g, the crystallinity percentage was calculated using the following equation:

$$Xc = \frac{\Delta H_f}{\Delta H_{f0}} \times 100$$

Table 3

The enthalpy of fusion and crystallinity percentage of the analyzed membranes.

Sample	Polymer percentage in sample - wt. %	Enthalpy of fusion - ΔHm [J/g] [J/g]	Crystallinity percentage - Xc [%]
CAm	100	33.2	56.46
CA/Zn5	95	31.6	53.73

The modified membrane has a lower crystallinity percentage compared to the neat one, probably due to an increase in the disorder degree of the cellulose acetate, generated by the interactions of the polymeric chains with the precipitated zinc compounds.

3.4 SEM

The commercial CA membranes are produced by impregnating pure cellulose acetate on a nonwoven support. Due to the technique used, they are composed of stacked polymeric layers, each layer being made up of polymeric strands, ordered in a honeycomb-like porous structure with approximate pore size ranging from 1 to 5 µm, as it can be observed in Fig 2a. After the impregnation with zinc acetate solution and the subsequent ammonia hydroxide treatment, the porosity gradually starts to decrease. This phenomenon may be attributed to the thickening of the polymeric strands due to the deposition of zinc-based compounds on their surface. Also, starting with a 2% zinc concentration, the polymeric layers seem to fuse together, forming a smooth compact structure, this indicating that the interactions between the cellulosic matrix and the zinc compounds lead to changes in the morpho-structural characteristics of the modified membranes.

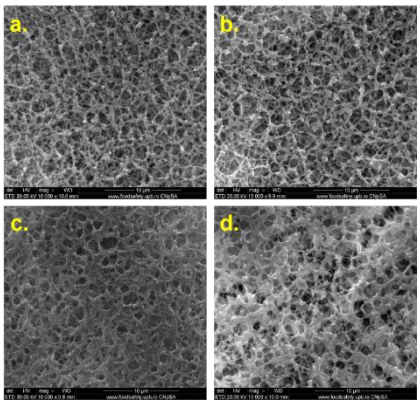

Fig. 4. SEM images of the CA membranes at 10000 X magnification – CAm (a), CA/Zn1 (b), CA/Zn2 (c), CA/Zn5 (d).

3.5 EDS

The main elements present in the CA/Zn5 membrane structure are, as expected, carbon, oxygen and zinc. The small peak attributed to gold is present due to the sample metallization process necessary for acquiring SEM images.

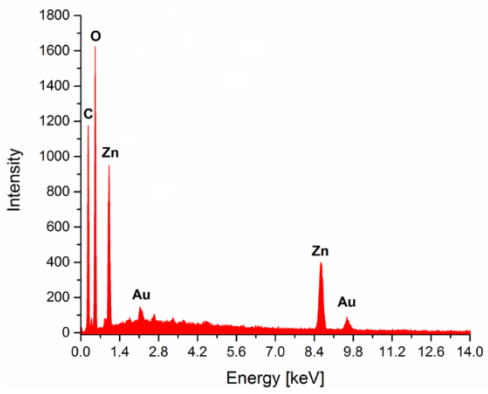

Fig. 5. The EDS spectrum of the CA/Zn5 membrane.

The EDS maps shows the spatial distribution of the elements in the sample. Carbon is represented with yellow, oxygen with light blue and zinc with green. Zinc is present in a high percentage, and it is evenly distributed throughout the cellulose acetate matrix, in the form of different zinc compounds, as observed in the FT-IR spectra. The membrane porosity and the amorphous structure of the precipitated zinc compounds have a positive effect on the distribution of zinc in the cellulose acetate network, no particle aggregation effect being noticed even at the highest zinc salt solution concentration used (5%).

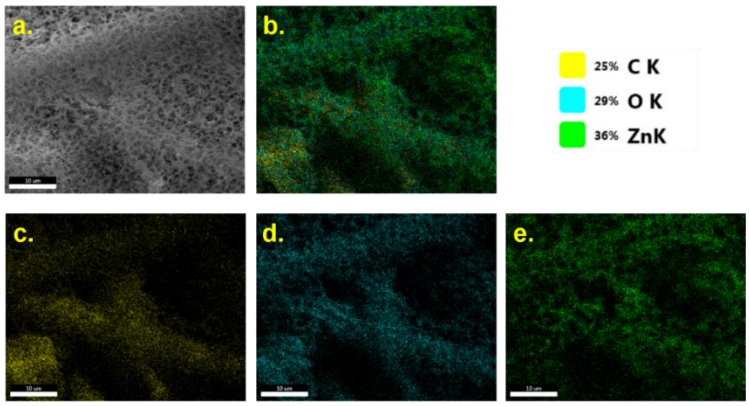

Fig. 6. EDS maps of the CA/Zn5 membrane – SEM image (a), full elemental map (b), carbon map (c), oxygen map (d), zinc map (e).

3.6 Swelling degree

The membranes presented a typical swelling kinetics: a rapid absorption phase in the first 8 hours followed by an equilibrium phase with no substantial changes in the next 40 hours. The total time period of the test was 48 hours. A decrease in the swelling degree can be observed for the modified membrane, probably due to the hydrophobicity of the zinc compounds and also to the lower membrane porosity. The average fluid uptake percentage is approximately 70% for the neat membrane and 32% for the zinc loaded one.

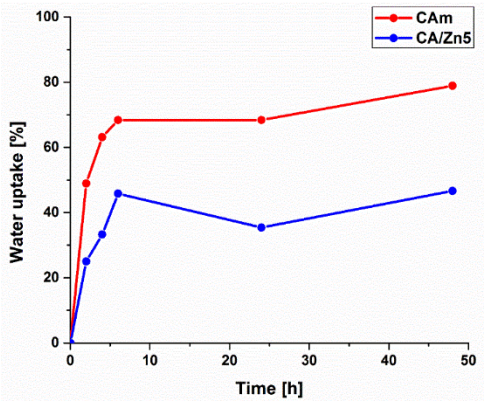

Fig. 7. Swelling degree characteristics of the CA membranes – neat (CAm) and 5% zinc (CA/Zn5).

3.7 Antibacterial activity

Qualitative assessment

The diameter of the inhibition area surrounding each sample was measured and expressed in millimeters (Fig. 9), the results being summarized in Table 4. In the case of the *Gram-positive* bacterial strain *S. Aureus*, the inhibition zone

diameter increased progressively from 7 to 16 mm, depending on the zinc content, which means that the amount of zinc compounds released from the modified membranes was high enough to reach the concentration required for the inhibition of bacterial growth. A lower bacterial sensitivity was observed in the case of the *Gram-negative P. aeruginosa*, changes in the inhibition zone diameter being noticed only in the case of the CA/Zn5 membrane. The sensitivity differences between the two tested bacterial strains are related to the distinctive cell wall structures of *Gram negative* and *Gram positive* bacteria, the latter ones having a higher susceptibility to antibacterial compounds [41].

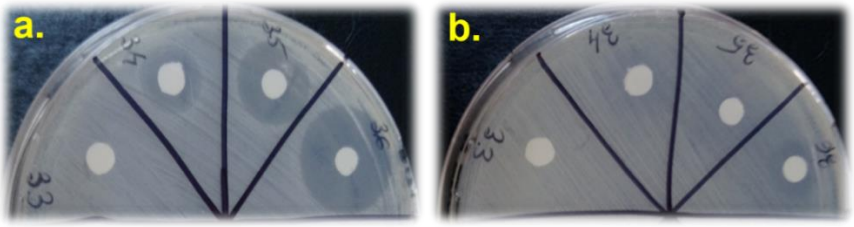

Fig. 8. Aspect of the growth inhibition areas for *S. Aureus* (a) and *P. Aeruginosa* (b): 33 - neat CA, 34 - CA/Zn1, 35 – CA/Zn2, 36 – CA/Zn5.

Table 4

Measured diameter of the growth inhibition areas for *S. Aureus* and *P. Aeruginosa*.

Sample	Inhibition zone diameter [mm]	
	***Staphylococcus aureus* ATCC 25923**	***Pseudomonas aeruginosa* ATCC 27853**
CAm	0	0
CA/Zn1	7	0
CA/Zn2	11	0
CA/Zn5	16	5

Semi-quantitative assessment

The bacterial growth inhibition effect of the tested membranes is indicated by a low turbidity of the microbial suspensions in the well plate, respectively by lower absorbance values compared to the bacterial growth witness (GW). The modified membranes show good antibacterial activity for both *S. Aureus* and *P. Aeruginosa*, the absorbance values being very close to the one of the sterility witnesses (SW, absorbance value = 0) especially at higher zinc contents (Fig. 10). Interestingly, in the case of *S. Aureus*, the absorbance value for the neat CA membrane is slightly above the one of the bacterial growth witnesses, this meaning that plain CA favors the microbial development. Also, the lowest absorbance value was recorded for the CA/Zn1 sample and unexpectedly, the absorbance increased proportionally to the zinc content. This anomalous behavior

is currently under investigation, but a presumptive explanation could be related to inhomogeneities in the zinc distribution throughout the membrane section used for this assessment. The antimicrobial action against *P. Aeruginosa* followed the expected trend, a higher zinc content resulting in a more effective inhibition of the bacterial growth.

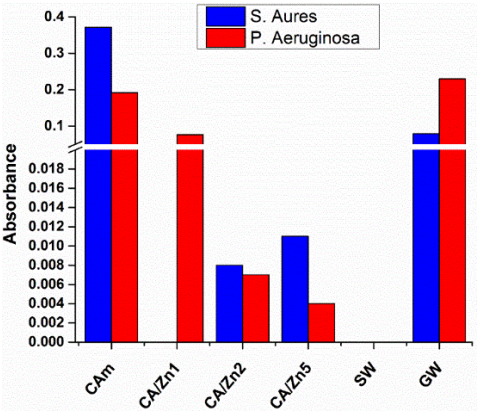

Fig. 9. Graphical representation of the absorbance values for the semi-quantitative assessment of the CA membranes growth inhibition capacity for *S. Aureus* and *P. Aeruginosa* bacterial strains.

Quantitative assessment

The microbial suspensions resulted from the semi-quantitative assessment were further used in the quantitative test. As it can be observed in Fig. 11, the viability of the bacterial cells decreased proportionally to the zinc content in the membranes this suggesting that the modified membranes could effectively kill bacteria in a concentration dependent manner. A significant growth inhibition of up to 10 logarithmic units was recorded for the CA/Zn5 membranes, particularly in the case of *S. Aureus*, compared to the neat cellulose acetate but also to the bacterial growth witness.

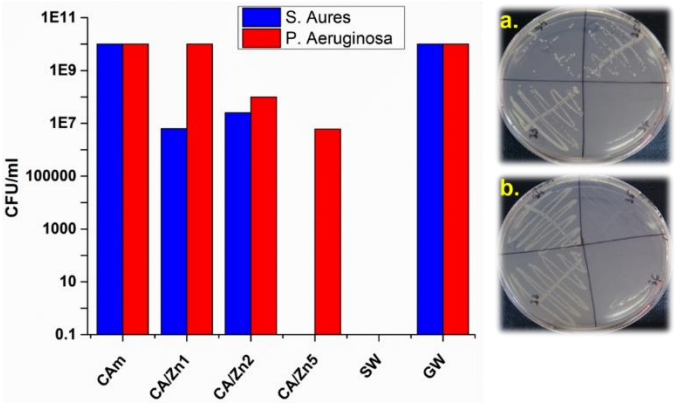

Fig. 10. Graphical representation of the CFU/ml values and the aspect of the inoculated microbial suspensions of *S. Aureus* (a) and *P. Aeruginosa*: 33 – neat CA, 34 – CA/Zn1, 35 – CA/Zn2, 36 – CA/Zn5.

4. Conclusions

This study presented a facile cellulose acetate membranes modification method based on impregnation with zinc salt solution followed by alkaline precipitation. FT-IR, SEM and EDS analysis revealed the successful loading with antibacterial zinc-based compounds, particularly zinc hydroxide, complex tetraaminezincate ions and zinc oxide, and their homogeneous distribution throughout the membranes structure. Also, the zinc loading did not significantly influence the thermal stability and swelling degree of cellulose acetate. From the antibacterial assessments, it can be concluded that the zinc loaded CA membranes have good antibacterial activity against both *Gram-positive* and *Gram-negative* bacterial strains, a higher zinc content resulting in a more pronounced microbial growth inhibition. These results indicate that modifying cellulose acetate membranes with zinc salts could be an effective method for the obtainment of wound dressings with favorable antibacterial properties.

R E F E R E N C E S

[1] Aslam B, Wang W, Arshad MI, Khurshid M, Muzammil S, Rasool MH, et al. Antibiotic resistance: a rundown of a global crisis. Infect Drug Resist 2018; 11:1645-58.

[2] Oprea M, Panaitescu DM. Nanocellulose Hybrids with Metal Oxides Nanoparticles for Biomedical Applications. Molecules (Basel, Switzerland) 2020; 25.

[3] Muhulet A, Tuncel C, Miculescu F, Pandele AM, Bobirica C, Voicu ȘI, et al. Synthesis and characterization of polysulfone–TiO_2 decorated MWCNT composite membranes by sonochemical method. Appl. Phys. A 2020; 126.

[4] Tariq S, Wani S, Rasool W, Shafi K, Bhat MA, Prabhakar A, et al. A comprehensive review of the antibacterial, antifungal and antiviral potential of essential oils and their chemical constituents against drug-resistant microbial pathogens. Microb. Pathog. 2019; 134:103580.

[5] Sharma C, Bhardwaj NK. Fabrication of natural-origin antibacterial nanocellulose films using bio-extracts for potential use in biomedical industry. Int. J. Biol. Macromol. 2020; 145:914-25.
[6] Liu F, Li X, Wang L, Yan X, Ma D, Liu Z, et al. Sesamol incorporated cellulose acetate-zein composite nanofiber membrane: An efficient strategy to accelerate diabetic wound healing. Int. J. Biol. Macromol. 2020; 149:627-38.
[7] Ullah A, Ullah S, Khan MQ, Hashmi M, Nam PD, Kato Y, et al. Manuka honey incorporated cellulose acetate nanofibrous mats: Fabrication and in vitro evaluation as a potential wound dressing. Int. J. Biol. Macromol. 2020; 155:479-89.
[8] Sun D, Babar Shahzad M, Li M, Wang G, Xu D. Antimicrobial materials with medical applications. Mater. Technol. 2015; 30:B90-B5.
[9] Bakhsheshi-Rad HR, Hadisi Z, Ismail AF, Aziz M, Akbari M, Berto F, et al. In vitro and in vivo evaluation of chitosan-alginate/gentamicin wound dressing nanofibrous with high antibacterial performance. Polym. Test. 2020; 82:106298.
[10] Naseri-Nosar M, Ziora ZM. Wound dressings from naturally-occurring polymers: A review on homopolysaccharide-based composites. Carbohydr. Polym. 2018; 189:379-98.
[11] Moeini A, Pedram P, Makvandi P, Malinconico M, Gomez d'Ayala G. Wound healing and antimicrobial effect of active secondary metabolites in chitosan-based wound dressings: A review. Carbohydr. Polym. 2020; 233:115839.
[12] Du H, Liu W, Zhang M, Si C, Zhang X, Li B. Cellulose nanocrystals and cellulose nanofibrils based hydrogels for biomedical applications. Carbohydr. Polym. 2019; 209:130-44.
[13] Raicopol MD, Andronescu C, Voicu SI, Vasile E, Pandele AM. Cellulose acetate/layered double hydroxide adsorptive membranes for efficient removal of pharmaceutical environmental contaminants. Carbohydr. Polym. 2019; 214:204-12.
[14] Oprea M, Voicu SI. Cellulose Composites with Graphene for Tissue Engineering Applications. Materials 2020; 13:5347.
[15] Voicu ŞI, Pandele AM, Tanasă E, Rughinis R, Crica L, Pilan L, et al. The impact of sonication time through polysulfone-graphene oxide composite films properties. Dig. J. Nanomater. Biostruct. 2013; 8:1389-94.
[16] Voicu SI, Thakur VK. Aminopropyltriethoxysilane as a linker for cellulose-based functional materials: New horizons and future challenges. Curr. Opin. Green Sustain. Chem. 2021; 30:100480.
[17] Palla-Papavlu A, Voicu SI, Dinescu M. Sensitive Materials and Coating Technologies for Surface Acoustic Wave Sensors. Chemosensors 2021; 9:105.
[18] Mohd N, Syed draman Sf, Salleh MSN, Yusof B. Dissolution of cellulose in ionic liquid: A review. AIP Conference Proceedings 2017; 1809:020035.
[19] Oprea M, Voicu SI. Cellulose Composites with Graphene for Tissue Engineering Applications. Materials 2020; 13:5347.
[20] Thakur VK, Voicu SI. Recent advances in cellulose and chitosan based membranes for water purification: a concise review. Carbohydr. Polym. 2016; 146:148-65.
[21] Oprea M, Voicu SI. Recent advances in composites based on cellulose derivatives for biomedical applications. Carbohydr. Polym. 2020; 247:116683.
[22] Zizovic I, Senerovic L, Moric I, Adamovic T, Jovanovic M, Krusic MK, et al. Utilization of supercritical carbon dioxide in fabrication of cellulose acetate films with anti-biofilm effects against Pseudomonas aeruginosa and Staphylococcus aureus. J. Supercrit. Fluids 2018; 140:11-20.
[23] Chen JC, Soden KJ. Anti-adhesion cellulose acetate wound dressing. Google Patents 2002; CA2246992C.

[24] Almoudi MM, Hussein AS, Abu Hassan MI, Mohamad Zain N. A systematic review on antibacterial activity of zinc against Streptococcus mutans. Saudi Dent. J. 2018; 30:283-91.
[25] Artifon W, Pasini SM, Valério A, González SYG, de Arruda Guelli Ulson de Souza SM, de Souza AAU. Harsh environment resistant - antibacterial zinc oxide/Polyetherimide electrospun composite scaffolds. Mater. Sci. Eng. C 2019; 103:109859.
[26] Ahmed R, Tariq M, Ali I, Asghar R, Noorunnisa Khanam P, Augustine R, et al. Novel electrospun chitosan/polyvinyl alcohol/zinc oxide nanofibrous mats with antibacterial and antioxidant properties for diabetic wound healing. Int. J. Biol. Macromol. 2018; 120:385-93.
[27] Holt BA, Gregory SA, Sulchek T, Yee S, Losego MD. Aqueous Zinc Compounds as Residual Antimicrobial Agents for Textiles. ACS Applied Mater. Interfaces 2018; 10:7709-16.
[28] Goswami M, Das AM. Synthesis and characterization of a biodegradable Cellulose acetate-montmorillonite composite for effective adsorption of Eosin Y. Carbohydr. Polym. 2019; 206:863-72.
[29] Ahmed F, Ayoub Arbab A, Jatoi AW, Khatri M, Memon N, Khatri Z, et al. Ultrasonic-assisted deacetylation of cellulose acetate nanofibers: A rapid method to produce cellulose nanofibers. Ultrason. Sonochem. 2017; 36:319-25.
[30] Das AM, Ali AA, Hazarika MP. Synthesis and characterization of cellulose acetate from rice husk: Eco-friendly condition. Carbohydr. Polym. 2014; 112:342-9.
[31] Voicu SI, Condruz RM, Mitran V, Cimpean A, Miculescu F, Andronescu C, et al. Sericin Covalent Immobilization onto Cellulose Acetate Membrane for Biomedical Applications. ACS Sustain. Chem. Eng. 2016; 4:1765-74.
[32] Luo Z, Cheng W, Chen H, Fu X, Peng X, Luo F, et al. Preparation and Properties of Enzyme-Modified Cassava Starch-Zinc Complexes. J. Agric. Food Chem. 2013; 61.
[33] Katepetch C, Rujiravanit R, Tamura H. Formation of nanocrystalline ZnO particles into bacterial cellulose pellicle by ultrasonic-assisted in situ synthesis. Cellulose 2013; 20.
[34] Thein M, Pung S, Azizan A, Itoh M. The role of ammonia hydroxide in the formation of ZnO hexagonal nanodisks using sol–gel technique and their photocatalytic study. J. Exp. Nanosci. 2014; 10:1-15.
[35] Kołodziejczak-Radzimska A, Markiewicz E, Jesionowski T. Structural Characterisation of ZnO Particles Obtained by the Emulsion Precipitation Method. J. Nanomater. 2012; 2012.
[36] Sajó E, Kótai L, Keresztury G, Gács I, Pokol G, Kristóf J, et al. Studies on the Chemistry of Tetraamminezinc(II) Dipermanganate ([Zn(NH3)4](MnO4)2): Low-Temperature Synthesis of the Manganese Zinc Oxide (ZnMn2O4) Catalyst Precursor. Helv. Chim. Acta 2008; 91:1646-58.
[37] Kayani Z, Iqbal M, Riaz S, Zia R, Naseem S. Fabrication and properties of zinc oxide thin film prepared by sol-gel dip coating method. Mat. Sci. Poland 2014; 33.
[38] Moafi HF, Shojaie AF, Zanjanchi MA. Photocatalytic self-cleaning properties of cellulosic fibers modified by nano-sized zinc oxide. Thin Solid Films 2011; 519:3641-6.
[39] De Campos E, Campos S, Roos A, Souza B, Schneider J, Uliana M, et al. Titanium Dioxide Dispersed on Cellulose Acetate and its Application in Methylene Blue Photodegradation. Polym. Polym. Compos. 2013; 21:423-30.
[40] Lin C-C, Li Y-Y. Synthesis of ZnO nanowires by thermal decomposition of zinc acetate dihydrate. Mater. Chem. Phys. 2009; 113:334-7.
[41] Exner M, Bhattacharya S, Christiansen B, Gebel J, Goroncy-Bermes P, Hartemann P, et al. Antibiotic resistance: What is so special about multidrug-resistant Gram-negative bacteria? GMS Hyg. Infect. Control 2017; 12:Doc05.